Chan, S. N.; Cong, J.; Lee, J. H. W.

Numerical Modeling of Geyser Formation by Release of Entrapped Air from Horizontal Pipe into Vertical Shaft

12th International Conference on Hydroscience & Engineering
Hydro-Science & Engineering for Environmental Resilience
November 6-10, 2016, Tainan, Taiwan.

Numerical Modeling of Geyser Formation by Release of Entrapped Air from Horizontal Pipe into Vertical Shaft

S.N. Chan, J. Cong, J.H.W. Lee
Department of Civil and Environmental Engineering, Hong Kong University of Science and Technology
Clear Water Bay, Hong Kong SAR, China

ABSTRACT

Geysers are explosive eruptions of air-water mixture from manholes in drainage systems. Due to urbanization and climate change, the design capacity of storm water drainage systems in many cities is often exceeded during extreme rainfall; rapid inflows into the drainage network can lead to air-water interactions that give rise to geysers - causing damages to the water infrastructure and threatening human lives. Although extensive research has revealed the role of entrapped air in causing large pressure transients in drainage tunnels, the mechanism of geyser formation remains elusive mainly due to the lack of detailed observations. In this study, an unsteady 3D computational fluid dynamics model is developed to simulate the pressure transients and air-water interactions during geyser events using the Volume-of-Fluid (VOF) technique. Model predictions of air-water interface in the vertical shaft are in good agreement with measurements by high-speed camera; the mechanism for the formation of geysers is elucidated.

KEY WORDS: Geyser; Urban drainage; Hydraulic transients; Air-water interaction; Taylor bubble, Volume-of-fluid, Numerical modeling

INTRODUCTION

Geysers are explosive eruptions of air-water mixture from manholes in drainage systems. Due to urbanization and climate change, the design capacity of storm water drainage systems in many cities is often exceeded during extreme rainfall; rapid inflows into the drainage network can lead to air-water interactions that give rise to geysers - causing damages to the water infrastructure and threatening human lives. In previous studies, geysers have been attributed to pressure surges caused by rapid inflows (e.g. Guo and Song 1991) and air-water interactions due to instabilities associated with the transition from gravity to pressurized flow in pipe systems (e.g. Li and McCorquodale 1999). The possibility that air pockets can give rise to significant pressures had also been demonstrated theoretically and experimentally (Martin 1976; Zhou et al. 2002a and 2002b). More recently, systematic investigations have advanced significantly our understanding of the flow caused by entrapped air in pipelines (Wright et al. 2011; Wright 2013; Vasconcelos and Wright 2006, 2008 and 2011). These experiments demonstrated the possibility of different types of air-water interactions as a function of riser and pipe diameters, and rate of increase of inflows into an existing pipeline partially filled with water.

While the previous studies have confirmed the role of entrapped air in causing large pressure transients, the mechanism of geyser formation remains elusive, mainly due to the lack of detailed observations and measurements of key variables - e.g. interface velocities and air pocket pressure. In particular, the physical mechanisms under which geysers are formed have not been conclusively reported or elucidated.

A comprehensive series of laboratory experiments has recently been performed on a physical model of a simplified drainage system (Cong et al. 2016; Cong 2016), which consists of a vertical riser and a horizontal pipe connected to a constant head tank. The system is filled with water; an air pocket is then released into the horizontal pipe and the trajectories of the air pockets in horizontal pipe and vertical riser are measured by videos and a high speed camera. Pressures are measured using pressure transducers near the pipe end and at the bottom of riser. Parameters considered include riser diameter, upstream head, and initial air pocket volume. From the experiments and physical considerations, the vertical air pocket motion in a geyser differs greatly from that of a Taylor bubble (Davies and Taylor 1950). The importance of the ratio of riser to pipeline diameter, and the volume of air in geyser formation was revealed by experiments and theory.

Computational fluid dynamics (CFD) modeling is useful in capturing greater details of the physical processes than 1D models based on the rigid column hypothesis. Zhou et al. (2011) performed 2D Volume of Fluid (VOF) calculations on the transient flow of an air pocket trapped in a pipeline; the computed pressure variation compared well with experimental measurements. Catano-Lopera et al. (2014) conducted 3D two-phase flow calculations to study the occurrences of geysers for a small section of the Chicago tunnel and reservoir plan (TARP) system. Although the surging of the air-water mixture in the vertical riser is demonstrated, the physics of the geyser flow in the riser cross-section remains unresolved. The previous numerical and experimental studies failed to offer a clear explanation of the mechanism of geyser flow.

This paper presents a CFD study on geyser events using the two-phase Volume-of-Fluid technique and the experimental configuration of Cong et al. (2016). The set-up of the CFD model will first be described. The computed detailed air-water interface motion in the vertical riser are presented and compared with experimental data. The mechanism for the formation of a geyser is elucidated for the first time along with the conditions that will likely lead to geyser events.

NUMERICAL MODEL

The Volume-of-Fluid (VOF) model can simulate two immiscible fluids (water and air) by solving a single set of momentum equations and tracking the volume fraction of each of the fluids throughout the domain. The tracking of the interface between the phases is accomplished by the solution of a continuity equation for the volume fraction of one of the phases. A single momentum equation is solved throughout the domain, and the resulting velocity field is shared among the phases. The density of air is related to the pressure using the ideal gas law. The turbulent viscosity is determined using the standard k-ε turbulence model. The VOF model in the ANSYS FLUENT 15 software is used for the simulation.

The model grid is configured the same as the experimental work of Cong et al. (2016) and Cong (2016). The physical model consists of a vertical riser and a horizontal pipe connected to a constant head tank. The pipe is 6.6 meter long with an inner diameter of D = 0.05m. A riser of height 1.8m of variable diameter D_r = 0.016-0.046m is connected to the pipe with a T-junction at x = 3.47m from the upstream. A number of PVC quarter-turn ball valves are used to separate the pipe into different sections to allow experiments with different air volume.

In the numerical model, the tunnel-riser system is discretized using about 100,000 boundary-fitted grid cells. A schematic diagram of the model is shown in Figure 1. The tunnel cross section is discretized using 25 cells in the diameter, with finer grid size approaching the tunnel wall. The riser diameter is discretized using about 50 cells, with smallest grid size of 0.1mm to capture the film flow around the air pocket. Height of the riser in the computational model is 3.0m, compared to the 1.8m height in the physical experiment, to confine the air pocket and water column in the riser. The T-junction of the tunnel-riser system is discretized using tetrahedral cells while the other parts using hexahedral cells (Fig. 1).

Numerical experiments were performed similar to the laboratory experiments described in Cong et al. (2016). In an experiment without external pressure (Series A), the riser and horizontal pipe is filled with water to an initial head of H_0; the downstream section of the pipe is an air pocket of length L_0 and volume $V_{air} = \pi L_0 D^2/4$. By closing a selected ball valve, air pockets of different initial lengths (or volumes) can be formed. Series B experiments are conducted with a pressurized pipe connected to a constant head tank with the initial water depth in the riser at the same level.

In the simulation, two riser diameters are tested: D_r = 16 and 40mm, with upstream pressure head H_0 = 0.88m. The length of initial pocket L_0 is 0.61 and 1.8m respectively for the two riser diameters. For Series A experiment, both ends of the tunnel is set as closed-end walls. For Series B experiments, the upstream end of the tunnel is prescribed as a pressure inlet with pressure = $\rho_w g H_0$ and volume fraction of water = 1, to simulate the effect of the upstream reservoir. The top of the riser is prescribed as a pressure outlet of zero (atmospheric) pressure and volume fraction of water = 0. A smooth wall is assumed for the pipe wall with roughness length of 10^{-3} mm.

The initial condition is set by prescribing a length of air of L_0 near the closed end of the tunnel and a water level of H_0 at the riser. The simulation starts at the time t = 0, equivalent to the opening of the ball valve in the experiment. It has to be noted that in the simulation the valve opening is instantaneous, while in the experiment the valve opening time is about 0.2s (Cong et al. 2016). Since the advection scheme of the VOF method is explicit, the Courant criteria has to be satisfied and the maximum $Cr = u\Delta t/\Delta x = 0.75$, an adaptive time step is used with minimum $\Delta t \approx 10^{-5}$s. The simulation is stopped when the upper air pocket bubble front has penetrated the free surface in the riser. The typical run time for a simulation on a quad-core computer (Intel i4790 3.6GHz CPU) is about 360-400 hours.

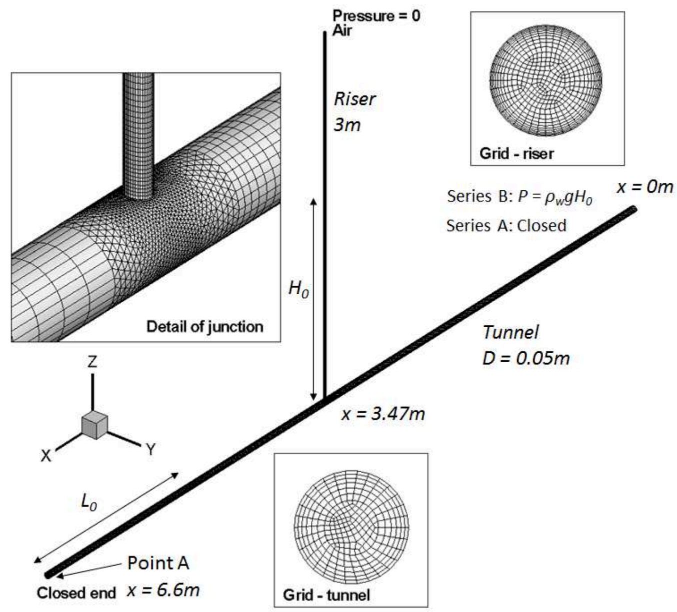

Figure 1 The model grid for 3D CFD simulation of geyser formation by release of an air pocket from horizontal pipe into a vertical riser.

RESULTS AND DISCUSSION

When the simulation starts (equivalent to the valve opening in the physical experiment), a density current is formed; the air pocket moves upstream in the upper half of the horizontal pipe, while the water propagates downstream. As the water reaches the downstream end, it is reflected to form an upstream moving front. The front of the air pocket continues to move towards the vertical riser.

Fig. 2a shows the pressure variation at Point A - the soffit of the downstream end of the pipe. The pressure increases sharply after the start of simulation due to the compression of the air pocket by the upstream pressure head. The volume of air in the system is estimated by summing up the product of the volume of computational cell and the air volume fraction inside. The reduction in air volume is about 10% at maximum (Fig. 2b), but it already creates the pressure increase of about 1.7 times the upstream head. The water level at the riser also fluctuates due to the pressure variation. The pressure and air volume variation is gradually damped due to the friction of the pipe and riser, till the air pocket reaches the riser. The pressure variation in general compares well with the measurement at the same locations in the physical experiment (Fig. 2a) and is consistent with the experimental studies of Zhou et al. (2002a) which shows that entrapped air pocket can lead to large pressure transients.

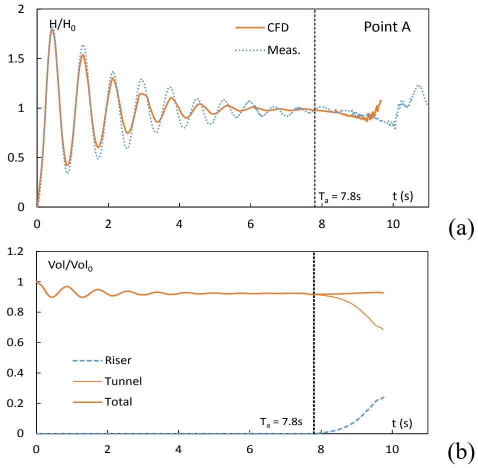

Figure 2 (a) Pressure and (b) total air volume for D_r = 16mm, H_0 = 0.88m, L_0 = 0.61m. T_a is the time when the air pocket arrives the riser.

Fig. 3 shows the simulation after the air pocket arrives at the vertical riser for D_r = 16mm with an upstream head (Series B), for which a geyser (an explosive release of a column of air-water mixture) is observed in the physical experiment. The air pocket arrives at the riser at T_a = 7.8s. Only part of the air enters the riser; while the remaining air keeps advancing upstream. Initially the air pocket rises in the riser steadily similar to a Taylor bubble (Davies and Taylor 1950). After some time, the nose of the air pocket undergoes a fast acceleration, with a velocity much greater than that of a Taylor bubble. The free surface is pushed by the air pocket to rise rapidly, until the bubble breaks at the free surface. A mixture of air and water finally enters the riser from the tunnel. In the physical experiment, the water is ejected out from the riser top, due to the smaller riser height (1.8m). The pressure in the tunnel initially drops steadily as the air pocket rises, but rises again when water enters the riser at about t = 9s (Fig. 2a). The total volume of air in the system remains more or less unchanged (Fig. 2b).

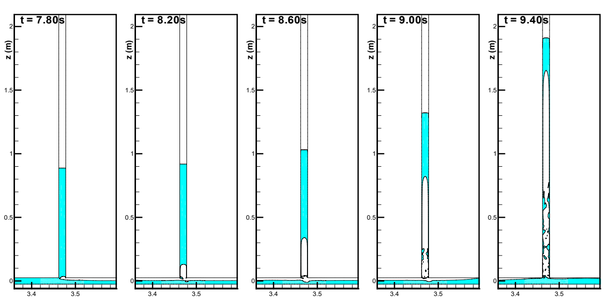

Figure 3 Predicted motion of air pocket in the vertical riser (D_r = 16mm, H_0 = 0.88m, L_0 = 0.61m).

Fig. 4a shows the computed level of the free surface in the riser Y_{fs} and the nose of the air pocket Y_{int} for the case of a geyser (D_r = 16mm). The predicted levels generally agree well with the measurement from high speed imaging, despite the greater predicted rise height due to the longer riser used in the simulation. The length of water column above the air pocket decreases due to the film flow around the air pocket, with a speed equal to the rising speed of the air pocket relative to the free surface. Initially the relative rising speed follows that of a Taylor bubble. At about 8.5s, there is a significant increase in the rising speed of Y_{fs} and Y_{int} (Fig 4b). On the other hand, the net rising speed of the air pocket is quite steady for the case without an upstream head (not shown), comparable to the Taylor bubble velocity:

$$V_{Taylor} = 0.345\sqrt{gD_r} \tag{1}$$

It can be noted that during a geyser event the computed average air pressure in the air pocket is much greater than the hydrostatic pressure due to the water column above (Fig. 4b). By the momentum conservation of the water column in the riser, the pressure difference creates an acceleration to push the water column out of the riser.

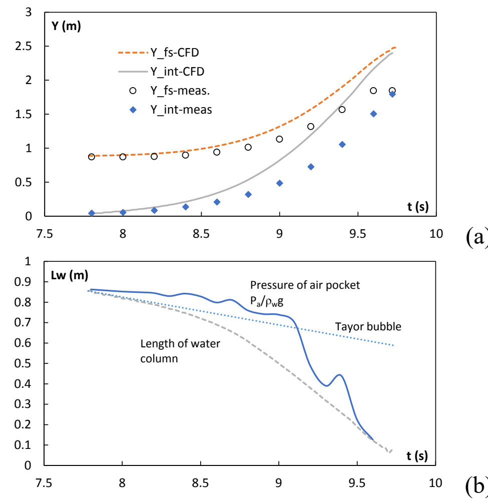

Figure 4 (a) Predicted air pocket front Y_{int} and free surface Y_{fs} in the riser (Series B); and (b) the pressure inside air pocket (D_r = 16mm).

Fig. 5 shows the simulated rise of air pocket for a larger D_r = 40mm with H_0 = 0.88m, L_0 = 1.8m (Series B). In this case geyser is not observed both with or without the upstream head. As the air pocket reaches the vertical riser, almost all air rises up in the riser and escape, instead of propagating upstream of the pipe. Both the air pocket and the free surface rises up more rapidly than that without an independent pressure head at upstream (Fig. 6a). An air-water mixture of churning flow is observed at the bottom of the riser and moves up since t = 5.3s. This influx of air-water mixture resulted in the rise of air pocket tip and the free surface level. The pressure in the air pocket in the riser is similar to the hydrostatic pressure induced by the water column above (Fig. 6b), thus there is no acceleration of the water column.

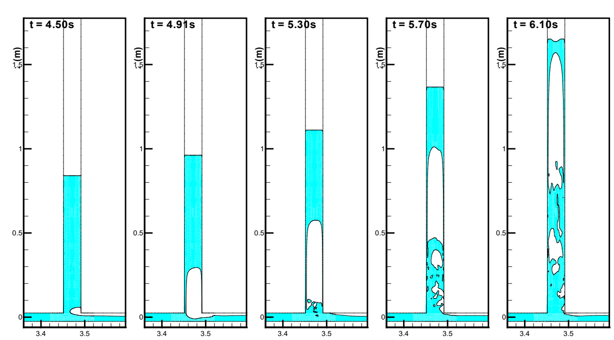

Figure 5 Predicted motion of air pocket in the vertical riser (D_r = 40 mm, H_0 = 0.88m, L_0 = 1.8m).

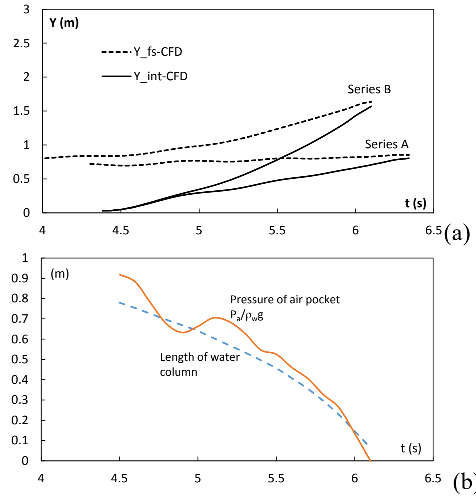

Figure 6 (a) Predicted levels of air pocket front Y_{int} and free surface Y_{fs} in the riser (Series A & B) and (b) the pressure inside air pocket (Series B, D_r = 40mm).

CONCLUSIONS

A numerical study on the physics of geyser events is conducted using a CFD model with the VOF technique. The predicted pressure variation, air-water interface and the free surface level in the riser compare well with experimental measurements. Geyser event occurs for the smaller riser diameter (D_r = 16mm) for the case with a prescribed independent upstream constant pressure head. The rising speed of both the air pocket tip and the free surface at the riser is much greater than those for the cases without an independent upstream pressure head. The pressure inside the air pocket in the riser is much greater than the hydrostatic pressure due to the water column above, resulting in the water column being rapidly pushed out of the riser, as observed in a geyser event. For the case with a large riser diameter (D_r = 40mm), the net rising speed of the air pocket relative to the free surface is similar to that of a Taylor bubble, without a net acceleration created by pressure difference. Further numerical study for examining the effect of riser diameter, air volume and other factors will be reported separately.

ACKNOWLEDGEMENTS

This research is supported by a grant from the Hong Kong Research Grants Council (RGC Project 16205114) and in part by a Smart Urban Water Supply Systems (SUWSS) project under the RGC Theme-Based Research Scheme (T21-602/15R).

REFERENCES

Catano-Lopera, Y.A., Tokyay, T.E., Martin, J.E., Schmidt, A.R., Lanyon, R., Fitzpatrick, K., Scalise, C.F., Garcia, M.H. (2014). Modeling of a transient event in the Tunnel and Reservoir Plan System in Chicago, Illinois. Journal of Hydraulic Engineering, 05014005/1-12

Cong, J., (2016). Experimental modeling of air-water interaction in horizontal pipe with vertical riser, M.Phil. thesis, Hong Kong University of Science and Technology.

Cong, J., Chan, S.N., Lee, J.H.W. (2016). Geyser Formation by Release of Entrapped Air from Horizontal Pipe into Vertical Shaft. Journal of Hydraulic Engineering (submitted).

Davies, R. M., and Taylor, G. I., (1950). The mechanics of large bubbles rising through extended liquids and through liquids in tubes, Proceedings of the Royal Society of London A: Mathematical, Physical and Engineering Sciences, 200, 375-390.

Guo, Q. and Song, C.C.S., (1990). Surging in urban storm drainage systems, Journal of Hydraulic Engineering, 116(12):1523-1537.

Li, J. and McCorquodale, A., (1999). Modeling mixed flow in storm sewers, Journal of Hydraulic Engineering, 125(11):1170-1180.

Martin, C.S., (1976). Entrapped air in pipelines, In Proc. 2nd Int. Conf. on Pressure Surges, Volume 2, pp.15-27, British Hydromechanics Research Association.

Vasconcelos, J. G. and Wright, S. J., (2006). Mechanisms for air pocket entrapment in stormwater storage tunnels, Proceedings of World Water and Environmental Resources Congress, Omaha, Nebraska, Paper 40856-14275.

Vasconcelos, J. G. and Wright, S. J., (2008). Rapid flow startup in filled horizontal pipelines, Journal of Hydraulic Engineering, ASCE, 134, 984-992.

Vasconcelos, J. G. and Wright, S. J., (2011). Geysering generated by large air pockets released through water-filled ventilation shafts, Journal of Hydraulic Engineering, ASCE, 137, 543-555.

Wright, S. J., and Lewis, J. W., and Vasconcelos, J. G., (2011). Geysering in rapidly filling storm-water tunnels, Journal of Hydraulic Engineering, ASCE, 137, 112-115.

Wright, S. J., (2013). Influence of Air Pocket Volume on Manhole Surge, (2013). Journal of Water Management Modeling, DOI: 10.14796/JWMM.R246-09

Zhou, F., Hicks, F. and Steffer, P.M. (2002a). Transient flow in a rapidly filling horizontal pipe containing trapped air, Journal of Hydraulic Engineering, 128(6): 625-634.

Zhou, F., Hicks, F. and Steffer, P.M. (2002b). Observations of air-water interaction in a rapidly filling horizontal pipe, Journal of Hydraulic Engineering, 128(6): 635-639.

Zhou, L., Liu, D.-Y. and Ou, C.-Q. (2011). Simulation of flow transients in a water filling pipe containing entrapped air pocket with VOF model. Engineering Applications of Computational Fluid Mechanics, 5(1), 127-140.